


 Cite this: *Nanoscale*, 2024, **16**, 9742



Received 21st March 2024,

Accepted 29th April 2024

DOI: 10.1039/d4nr01261e

[rsc.li/nanoscale](https://rsc.li/nanoscale)

## Consecutive one-pot alkyne semihydrogenation/alkene dioxygenation reactions by Pt(II)/Cu(II) single-chain nanoparticles in green solvent†

 Jokin Pinacho-Olaciregui,<sup>a,b</sup> Ester Verde-Sesto,<sup>a,c</sup> Daniel Taton <sup>b</sup> and José A. Pomposo <sup>a,c,d</sup>

**Heterobimetallic Pt(II)/Cu(II) single-chain polymer nanoparticles (SCNPs) were sequentially synthesized from a polymeric precursor featuring both  $\alpha$ -diazo- $\beta$ -ketoester and naked  $\beta$ -ketoester functional groups. Photoactivated carbene generation at  $\lambda_{\text{exc}} = 365$  nm from  $\alpha$ -diazo- $\beta$ -ketoester moieties was triggered for bonding Pt(II) ions from dichloro(1,5-cyclooctadiene)Pt(II) to the polymeric precursor, whereas Cu(II) ions were subsequently incorporated via Cu(II)-( $\beta$ -ketoester)<sub>2</sub> complex formation using Cu(II) acetate. Both intrachain Pt(II) bonding and Cu(II) complexation were found to contribute to the folding of the polymeric precursor generating Pt(II)/Cu(II)-SCNPs as evidenced by infrared spectroscopy, size exclusion chromatography and dynamic light scattering. These heterobimetallic SCNPs proved highly efficient as soft nanocatalysts for the consecutive one-pot alkyne semihydrogenation/alkene dioxygenation reactions at room temperature in *N*-butylpyrrolidone, as a non-toxic alternative solvent to *N,N*-dimethylformamide.**

Metal–ligand coordination allows intramolecular folding of ligand-decorated discrete synthetic polymer chains to metallofolded single-chain polymer nanoparticles (SCNPs).<sup>1</sup> SCNPs are intra-chain cross-linked single polymer chains with manifold promising applications, mainly as catalysts, nanosensors and drug nanocarriers.<sup>2,3</sup> In general, intramolecular folding of the isolated synthetic chains generates locally compact zones within the SCNPs for efficient immobilization of catalytic active species, luminophores or drugs.<sup>4</sup> To some extent, the intrachain folding of discrete synthetic polymer chains to

SCNPs resembles the folding of certain proteins to their precise functional conformation (*i.e.*, native state).<sup>5</sup> In particular, metallo-folded SCNPs leverage the dual role played by the metal: as a folding element *via* intra-chain metal–ligand coordination, and as an immobilized functional center for subsequent catalysis.<sup>6</sup> The number and catalytic applications of metallo-folded SCNPs as enzyme-mimetic nanoentities have grown significantly in recent years.<sup>7,8</sup> In a seminal work, Terashima *et al.* reported Ru-containing amphiphilic SCNPs to catalyse the reduction of cyclohexanone to cyclohexanol in water.<sup>9</sup> Pomposo *et al.* pioneered the introduction of metallofolded Cu(II)-containing SCNPs showing catalytic selectivity in alkyne homocoupling reactions,<sup>6</sup> and single-chain globules mimicking the morphology and polymerase activity of metalloenzymes.<sup>10</sup> He *et al.* prepared metallo-folded SCNPs containing Ni-thiolate complexes showing excellent thermal stability under aerobic conditions and excellent activity and selectivity during the photocatalytic reduction of CO<sub>2</sub> to CO.<sup>11</sup> Zimmerman *et al.* developed “clickase” SCNPs displaying enzyme-like “click” catalysis *in vivo* and enabling efficient cell surface glycan editing.<sup>12</sup> Taton *et al.* reported SCNPs containing Ag(I)-*N*-heterocyclic carbene (NHC) linkages as NHC pre-catalysts for the benzoin condensation reaction.<sup>13</sup> Yang *et al.* synthesized metal-containing SCNPs in concentrated solutions at room temperature (*r.t.*) by introducing electrostatic repulsion and intra-chain crosslinking by coordination with Cu(II) or Fe(II) or Fe(III) ions.<sup>14</sup> Tan *et al.* synthesized enzyme-mimetic SCNPs with chiral Fe(II)-oxazoline complexes for efficient asymmetric sulfa-Michael addition of thiols to  $\alpha,\beta$ -unsaturated ketones in water at *r.t.*<sup>15</sup> More recently, Pomposo *et al.* developed a method to upcycling poly(vinyl chloride) (PVC) waste to efficient catalytic Cu(II)-containing SCNPs.<sup>16</sup> Current advances in catalysis utilizing SCNPs have been recently reviewed by the Barner-Kowollik team.<sup>17</sup>

However, introduction of at least two distinct metal species in SCNPs although highly desirable is still synthetically challenging, since it requires designing a polymer chain able to complex both metal species while maintaining their orthogonality. In a pioneering work, Lemcoff *et al.* synthesized Rh(I)/

<sup>a</sup>Centro de Física de Materiales (CSIC – UPV/EHU) – Materials Physics Center MPC, P<sup>o</sup> Manuel Lardizabal 5, E-20018 Donostia, Spain.

E-mail: josetxo.pomposo@ehu.es

<sup>b</sup>Laboratoire de Chimie des Polymères Organiques (LCPO), Université de Bordeaux INP-ENSCBP, 16 av. Pey Berland, 33607 Pessac cedex, France

<sup>c</sup>IKERBASQUE – Basque Foundation for Science, Plaza Euskadi 5, E-48009 Bilbao, Spain

<sup>d</sup>Departamento de Polímeros y Materiales Avanzados: Física, Química y Tecnología. University of the Basque Country (UPV/EHU), P<sup>o</sup> Manuel Lardizabal 3,

E-20800 Donostia, Spain

† Electronic supplementary information (ESI) available. See DOI: <https://doi.org/10.1039/d4nr01261e>



Ir(I) SCNPs although their catalytic properties were not evaluated.<sup>18</sup> Subsequently, Barner-Kowollik *et al.* synthesized heterobimetallic Eu(III)/Pt(II)-SCNPs<sup>19</sup> and Au(I)/Y(III)-SCNPs<sup>20</sup> in which only one of the two metal ions, Pt(II) or Au(I), was used for catalysis, while the other was employed for sensing or intrachain folding (Eu(III) or Y(III), respectively). More recently, the same group decorated SCNPs folded through ferrocene units with Pd(II) atoms, which proved to be an active catalyst for the intramolecular hydroamination of an aminoalkyne.<sup>21</sup>

Advanced heterobimetallic nanocatalysts for carrying out multistep chemical processes in a single reaction vessel are currently of great interest in academia and industry.<sup>22</sup> Often, however, major costs of many consumer products synthesized in multistep processes are incurred in the purification and isolation of intermediates.<sup>23</sup> Additionally, replacement of toxic organic solvents by green solvents has attracted significant interest.<sup>24</sup> To the best of our knowledge, bimetallic SCNPs that would allow consecutive one-pot reactions to be performed in a green solvent have not been reported. To fill this gap, we report herein the proof of concept of heterobimetallic SCNPs through the synthesis of Pt(II)/Cu(II)-SCNPs, since these SCNPs

could show synergistic effects for catalysis and other applications. We show that these can serve as advanced soft nanocatalysts to perform consecutive one-pot alkyne semihydrogenation/alkene dioxygenation reactions in *N*-butylpyrrolidone (NBP) as a green solvent.

The synthetic procedure followed in this work to produce Pt(II)/Cu(II)-SCNPs is depicted schematically in Fig. 1. Initially, the monomers (2-acetoacetoxy)ethyl methacrylate (AEMA) and methyl methacrylate (MMA) were copolymerized *via* reversible addition fragmentation chain-transfer (RAFT) polymerization<sup>6</sup> yielding the random copolymer P0 (Fig. 1A). Subsequently, P0 with a content of  $\beta$ -ketoester functional groups of 30 mol%, a weight-average molecular weight of  $M_w = 73.6$  kDa and a narrow dispersity of  $D = 1.17$  was post-functionalized with 19 mol% of  $\alpha$ -diazo- $\beta$ -ketoester functional motifs using *p*-carboxybenzenesulfonazide (*p*-CBSA) as the diazo transfer reagent<sup>25</sup> leaving 11 mol%  $\beta$ -ketoester functional groups unreacted (see Fig. 1B and ESI†). Upon the diazo transfer reaction, the resulting polymeric precursor P1 showed  $M_w = 75.3$  kDa and  $D = 1.15$ , in very good agreement with the expected  $M_w$  (75.4 kDa) based on its chemical composition.

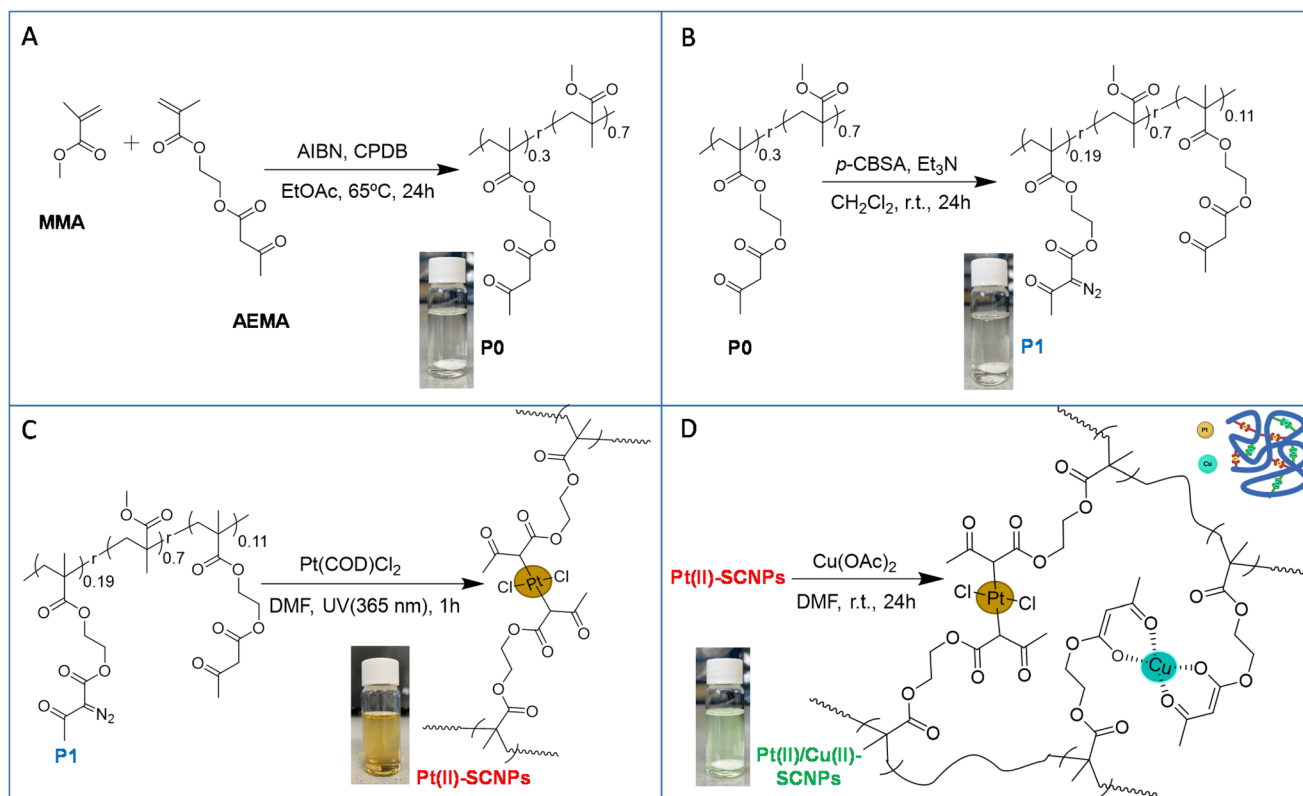


**Fig. 1** Schematic illustration of the synthesis of Pt(II)/Cu(II)-SCNPs: (A) Preparation of a random copolymer P0 containing naked  $\beta$ -ketoester functional groups (30 mol%) *via* reversible addition fragmentation chain-transfer (RAFT) polymerization (MMA = methyl methacrylate; AEMA = (2-acetoacetoxy)ethyl methacrylate; AIBN = azobisisobutyronitrile; CPDB = 2-cyanoprop-2-yl-dithiobenzoate; EtOAc = ethyl acetate). (B) Decoration of P0 with  $\alpha$ -diazo- $\beta$ -ketoester functional groups (19 mol%) to give polymeric precursor P1 (*p*-CBSA = *p*-carboxybenzenesulfonazide; Et3N = trimethylamine; CH2Cl2 = dichloromethane). (C) Folding of precursor P1 at high dilution *via* photoactivated carbene generation at  $\lambda_{\text{exc}} = 365$  nm in the presence of dichloro(1,5-cyclooctadiene)Pt(II) (Pt(COD)Cl2) to generate Pt(II)-SCNPs (DMF = dimethylformamide). (D) Additional folding of Pt(II)-SCNPs at high dilution *via* Cu(II) complexation by residual  $\beta$ -ketoester functional groups of Pt(II)-SCNPs (11 mol%) to give heterobimetallic Pt(II)/Cu(II)-SCNPs (Cu(OAc)2 = Cu(II) acetate).



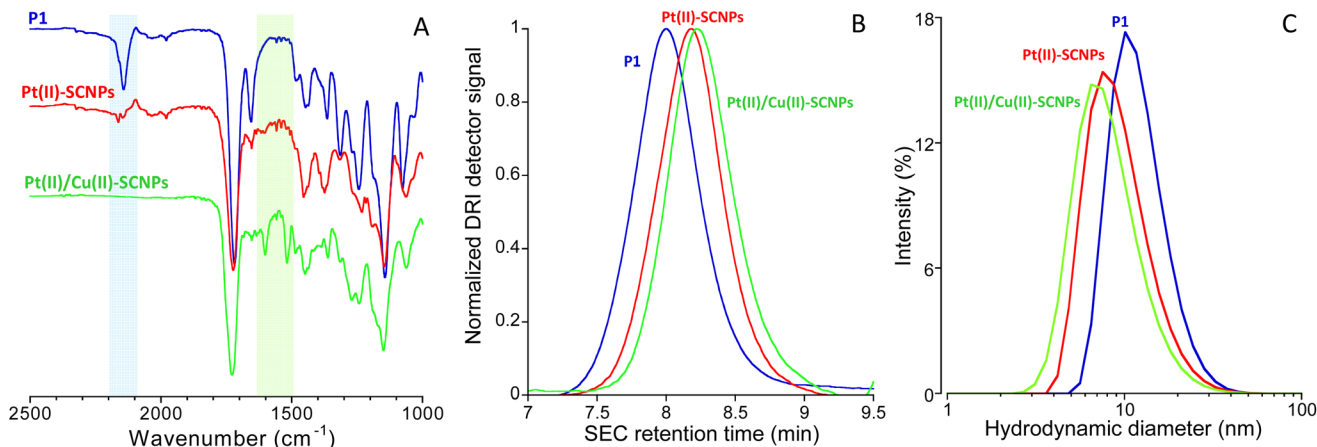


**Fig. 2** (A) Infrared (IR) spectra of polymeric precursor **P1**, **Pt(II)-SCNPs** and **Pt(II)/Cu(II)-SCNPs**. (B) Size exclusion chromatography (SEC) traces (differential refractive index (DRI) detector, DMF, 1 mL min<sup>-1</sup>) of **P1**, **Pt(II)-SCNPs** and **Pt(II)/Cu(II)-SCNPs**. (C) Dynamic light scattering (DLS) size distributions of **P1**, **Pt(II)-SCNPs** and **Pt(II)/Cu(II)-SCNPs** (see ESI† for details).

Infrared (IR) spectroscopy measurements confirmed the appearance of the characteristic infrared vibration band of the diazo moieties centred at  $\nu \approx 2200 \text{ cm}^{-1}$  (Fig. 2A). Heterobimetallic **Pt(II)/Cu(II)-SCNPs** were sequentially synthesized from **P1** containing both  $\alpha$ -diazo- $\beta$ -ketoester and unreacted  $\beta$ -ketoester functional groups. Thus, **P1** was first irradiated with UV light at  $\lambda_{\text{exc}} = 365 \text{ nm}$  at high dilution in the presence of dichloro(1,5-cyclooctadiene)Pt(II) (**Pt(COD)Cl<sub>2</sub>**) to generate the highly reactive carbene species from the  $\alpha$ -diazo- $\beta$ -ketoester functional groups and to promote intrachain cross-linking *via* Pt(II) bonding (see Fig. 1C).

Successful folding of **P1** to **Pt(II)-SCNPs** was confirmed through size exclusion chromatography (SEC) and dynamic light scattering (DLS) measurements, whereas the IR spectrum of **Pt(II)-SCNPs** showed the disappearance of the characteristic diazo IR vibration band after 1 h of UV irradiation (see

Fig. 2A). SEC results showed an increase in retention time, hence, a reduction in hydrodynamic size for the **Pt(II)-SCNPs** when compared to **P1** (Fig. 2B). The average hydrodynamic diameter of **P1**,  $D_h = 12.5 \text{ nm}$  as determined by DLS, was found to decrease to  $D_h = 9.9 \text{ nm}$  upon formation of the **Pt(II)-SCNPs** (Fig. 2C). In a final step, Cu(II) ions were incorporated using Cu(II) acetate<sup>6</sup> to form – in an orthogonal manner – Cu(II)-( $\beta$ -ketoester)<sub>2</sub> complexes from free  $\beta$ -ketoester functional groups of the **Pt(II)-SCNPs** (11 mol%) affording the heterobimetallic **Pt(II)/Cu(II)-SCNPs** (see Fig. 1D). Successful (additional) folding of **Pt(II)-SCNPs** into **Pt(II)/Cu(II)-SCNPs** was revealed by SEC (Fig. 2B) and DLS (Fig. 2C) analyses. The average hydrodynamic diameter of **Pt(II)/Cu(II)-SCNPs** was found to be  $D_h = 8.6 \text{ nm}$ . The less pronounced reduction in hydrodynamic size upon the second folding event can be attributed to the reduced degrees of freedom available after

**Table 1** Comparison of **Pt(II)/Cu(II)-SCNPs** to different control catalysts for consecutive alkyne semihydrogenation/alkene dioxygenation reactions at r.t. (see ESI†)

| Entry | Catalyst                                      | Solvent | Conv. of 1a (%) | Yield of 2a (%) | Yield of 3a (%) |
|-------|---|---------|-----------------|-----------------|-----------------|
| 1     | Pt(COD)Cl <sub>2</sub>                        | DMF     | 91              | 60              | —               |
| 2     | Cu(OAc) <sub>2</sub>                          | DMF     | —               | —               | —               |
| 3     | Pt(COD)Cl <sub>2</sub> + Cu(OAc) <sub>2</sub> | DMF     | 91              | 58              | 62              |
| 4     | P1-SCNPs <sup>a</sup>                         | DMF     | —               | —               | —               |
| 5     | Pt(II)-SCNPs                                  | DMF     | ≥99             | 90              | —               |
| 6     | Cu(II)-SCNPs <sup>b</sup>                     | DMF     | —               | —               | —               |
| 7     | Pt(II)-SCNPs + Cu(II)-SCNPs                   | DMF     | ≥99             | 93              | 82              |
| 8     | Pt(II)/Cu(II)-SCNPs                           | DMF     | ≥99             | 95              | 84              |
| 9     | Pt(II)/Cu(II)-SCNPs                           | NBP     | ≥99             | 95              | 80              |

<sup>a</sup> Synthesized as a control from **P1** according to the conditions provided in Fig. 1C without Pt(COD)Cl<sub>2</sub>. <sup>b</sup> Synthesized as a control from **P1-SCNPs** (entry 4) according to the conditions of Fig. 1D (NHPI = *N*-hydroxyphthalimide).



the first Pt(II)-induced compaction.<sup>26</sup> Complexation of Cu(II) ions by the residual  $\beta$ -ketoester groups was confirmed from the IR spectrum of the Pt(II)/Cu(II)-SCNPs. Fig. 2A indeed shows the characteristic vibration bands located at *ca.* 1600  $\text{cm}^{-1}$  (stretching C=O vibration, enol tautomer bonded to Cu) and *ca.* 1515  $\text{cm}^{-1}$  (stretching C=C vibration, enol tautomer bonded to Cu).<sup>6</sup> Inductively coupled plasma-mass spectrometry (ICP-MS) measurements showed a content of Pt(II) and Cu(II) ions in the Pt(II)/Cu(II)-SCNPs of 9.7  $\mu\text{g mg}^{-1}$  and 9.5  $\mu\text{g mg}^{-1}$ , respectively (see ESI†).

With the Pt(II)/Cu(II)-SCNPs in hand, we envisioned to use them as advanced soft nanocatalysts for consecutive one-pot (incompatible) reactions. To this end, we targeted the preparation of  $\beta$ -keto-*N*-alkoxyphthalimides, known intermediates of

great utility for the pharmaceutical and agricultural industries,<sup>27</sup> by using phenylacetylene substrates.

Table 1 shows a comparison of Pt(II)/Cu(II)-SCNPs with different control catalysts for the consecutive one-pot phenylacetylene (**1a**) semihydrogenation/styrene (**2a**) dioxygenation with air and *N*-hydroxyphthalimide (NHPI) at r.t. to give the  $\beta$ -keto-*N*-alkoxyphthalimide **3a** as the target product (see ESI†). With Pt(COD)Cl<sub>2</sub> (1 mol% Pt(II)) **1a** was transformed into **2a** in DMF with 60% yield, along with a large portion of **1a** completely hydrogenated to ethylbenzene (Table 1, entry 1). As expected, Cu(OAc)<sub>2</sub> (1 mol% Cu(II)) proved inefficient for the semihydrogenation of **1a** (Table 1, entry 2). A combination of Pt(COD)Cl<sub>2</sub> for the semihydrogenation reaction, and subsequently adding Cu(OAc)<sub>2</sub> for the dioxygenation reaction

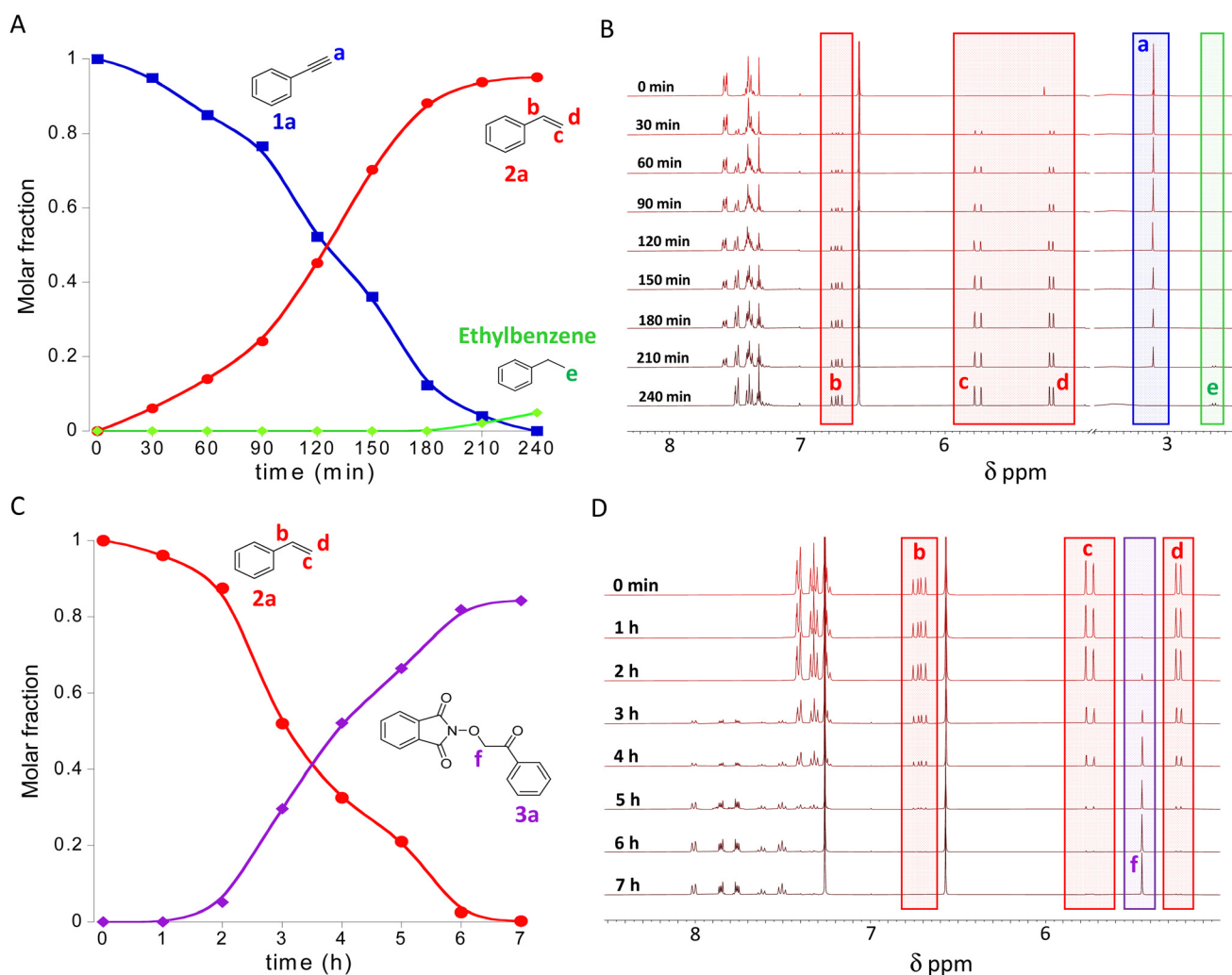


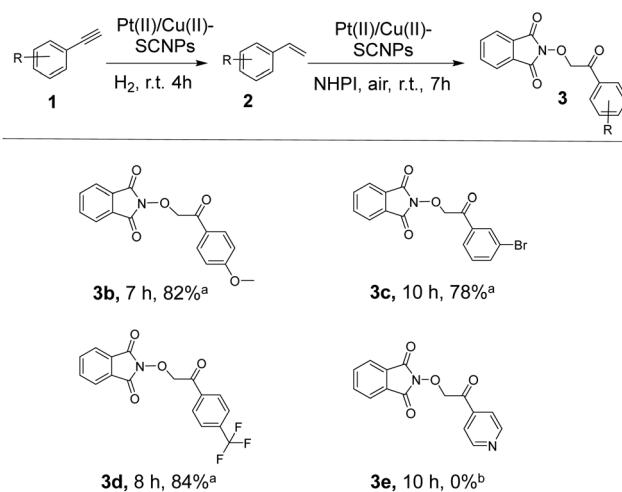
**Fig. 3** Consecutive one-pot alkyne semihydrogenation/alkene dioxygenation reactions catalysed by Pt(II)/Cu(II)-SCNPs in NBP at r.t.: (A) Evolution of the concentration of phenylacetylene (**1a**), styrene (**2a**) and ethylbenzene (secondary product) during the alkyne semihydrogenation reaction. (B) Reaction kinetics of the semihydrogenation reaction as followed by <sup>1</sup>H NMR spectroscopy through the disappearance of alkyne proton of **1a** denoted as **a**, and the concomitant appearance of the vinylic protons denoted as **b**, **c** and **d** of **2a**. Notice the presence of a small peak (denoted as **e**) coming from ethylbenzene after 210 min of reaction time. (C) Evolution of the amount of intermediate **2a** and product **3a** (2-(2-oxo-2-phenylethoxy)isoindoline-1,3-dione) during the dioxygenation reaction with air and *N*-hydroxyphthalimide (NHPI). (D) Reaction kinetics of the dioxygenation of intermediate **2a** as followed by <sup>1</sup>H NMR spectroscopy through the disappearance of the vinylic protons of **2a**, and the simultaneous appearance of the methylene protons denoted as **f** of **3a**.



gives a yield of **2a** and **3a** of 58% and 62%, respectively (Table 1, entry 3). **Pt(II)**-SCNPs (*i.e.*, 0.13 mol% Pt(II)) provided **2a** in 90% yield (Table 1, entry 5) whereas both **P1**-SCNPs synthesized—as a control—from **P1** without Pt(COD)Cl<sub>2</sub> and **Cu(II)**-SCNPs synthesized also as a control from **P1**-SCNPs, were totally inefficient (Table 1, entries 4 and 6). A combination of **Pt(II)**-SCNPs for the semihydrogenation reaction, and subsequently addition of **Cu(II)**-SCNPs (0.41 mol% Cu(II)) for the dioxygenation reaction provided **2a** and **3a** in 93% and 82% yield, respectively (Table 1, entry 7). Remarkably, the heterobimetallic **Pt(II)/Cu(II)**-SCNPs (0.14 mol% Pt(II) and 0.43 mol% Cu(II)) allowed the consecutive one-pot semihydrogenation/dioxygenation reaction to be carried out in DMF with exceptional selectivity and yield (Table 1, entry 8). Moreover, a similar efficiency and selectivity was found for the heterobimetallic **Pt(II)/Cu(II)**-SCNPs when the consecutive one-pot semihydrogenation of **1a**/dioxygenation of **2a** with air and NHPI was carried out in NBP as a green solvent to replace toxic DMF.

Fig. 3A shows the transformation of **1a** into **2a** over time during the semihydrogenation reaction in NBP, as monitored by <sup>1</sup>H NMR spectroscopy. The kinetics of this reaction was followed through the disappearance of the alkyne proton of **1a**, denoted as **a** in Fig. 3B and the concomitant appearance of the vinylic protons, denoted as **b**, **c** and **d** of **2a** (Fig. 3B). In the late stages, *i.e.*, after 210 min of reaction time, hydrogenation of **2a** to ethylbenzene (secondary product) takes place (see Fig. 3B). After 4 h of reaction time, the conversion of **1a** reached completion with a final yield in **2a** of 95%. The turnover number (moles of product per mole of catalyst, TON) of the **Pt(II)/Cu(II)**-SCNPs in the semihydrogenation reaction was TON = 679 (a value 10 times higher than that of Pt(COD)Cl<sub>2</sub> at 1 mol% Pt(II), see ESI, Table S3†). Without isolation of **2a**, the crude product of the semi-hydrogenation reaction containing the bimetallic **Pt(II)/Cu(II)**-SCNPs was used for the dioxygenation of **2a** with air and NHPI at r.t. in the same reaction vessel. Fig. 3C illustrates the consumption of **2a** and the generation of the β-keto-*N*-alkoxyphthalimide **3a**, as the target product, over reaction time. Also in this case, the kinetics of the dioxygenation reaction in NBP was directly monitored by <sup>1</sup>H NMR spectroscopy through the disappearance of the vinylic protons, denoted as **b**, **c** and **d** of **2a** (Fig. 3D) and the simultaneous appearance of the methylene protons denoted as **f** in Fig. 3D of **3a**. After 7 h of reaction, the conversion of **2a** was nearly complete and the yield of **3a** was 80%. The turnover number of the **Pt(II)/Cu(II)**-SCNPs in the dioxygenation reaction was TON = 186. This value is 30-fold higher than that corresponding to the classical procedure<sup>27</sup> involving Cu(OAc)<sub>2</sub> as catalysts (see Table S3†).

Finally, we investigated the substrate scope of the consecutive one-pot alkyne semihydrogenation/alkene dioxygenation reactions catalysed by **Pt(II)/Cu(II)**-SCNPs in NBP (see Scheme 1). Substituted phenylacetylene at the *para*-position with a methoxy group gave the β-keto-*N*-alkoxyphthalimide **3b** in 82% isolated yield. The reaction of phenylacetylene bearing a bromine atom at *meta*-position produced the corresponding β-keto-*N*-alkoxyphthalimide **3c** in 78% isolated yield. The intro-



**Scheme 1** Substrate scope of the consecutive one-pot alkyne semihydrogenation/alkene dioxygenation reactions catalysed by **Pt(II)/Cu(II)**-SCNPs in NBP at r.t. <sup>a</sup> Isolated yield. <sup>b</sup> Dioxygenation of intermediate **2e** did not take place.

duction of a trifluoromethyl substituent in phenylacetylene at the *para*-position afforded the β-keto-*N*-alkoxyphthalimide **3d** in 84% isolated yield. In contrast, 4-ethynylpyridine failed to react under our reaction conditions during the dioxygenation reaction, which we attribute to the deactivation of the Cu(II) catalytic sites induced by the presence of the nitrogen atom in the aromatic ring. Further work—which is outside the scope of this communication—is guaranteed to gain insight into the complete reaction mechanism (a tentative mechanism is provided in Table S4†).

## Conclusions

We report bimetallic SCNPs as highly efficient soft nanocatalysts allowing consecutive one-pot (incompatible) reactions to be performed at r.t. in a green solvent. For this purpose, a polymeric precursor, **P1**, containing both α-diazo-β-ketoester and naked β-ketoester functional motifs was rationally designed. Pt(II) and Cu(II) ions were sequentially added not only to trigger intra-chain folding of **P1** chains at high dilution, but also to install two distinct type of metallic species for consecutive catalytic reactions. Efficient compaction was revealed by combining IR, SEC and DLS measurements, yielding catalytically active **Pt(II)/Cu(II)**-SCNPs. This unique heterobimetallic soft nanocatalyst was shown to be highly efficient for consecutive one-pot alkyne semihydrogenation/alkene dioxygenation reactions at r.t. in NBP, as a non-toxic alternative solvent to DMF, affording β-keto-*N*-alkoxyphthalimides as intermediates of great utility for the pharmaceutical and agricultural industries. Critically, this work paves the way to multi-step chemical reactions in a single reaction vessel with complex multi-metallic SCNPs as advanced nanocatalysts.



## Conflicts of interest

There are no conflicts to declare.

## Acknowledgements

We gratefully acknowledge Grant PID2021-123438NB-I00 funded by MCIN/AEI/10.13039/501100011033 and “ERDF A way of making Europe”, Grant TED2021-130107A-I00 funded by MCIN/AEI/10.13039/501100011033 and Unión Europea “NextGenerationEU/PRTR” and Grant IT-1566-22 from Eusko Jaurilaritza (Basque Government). E.V.-S. acknowledges financial support from RyC program (RYC2022-037590-I). The authors sincerely thank Davide Arena for technical support.

## References

- 1 S. Mavila, C. E. Diesendruck, S. Linde, L. Amir, R. Shikler and N. G. Lemcoff, *Angew. Chem., Int. Ed.*, 2013, **52**, 5767.
- 2 E. Verde-Sesto, A. Arbe, A. J. Moreno, D. Cangialosi, A. Alegría, J. Colmenero and J. A. Pomposo, *Mater. Horiz.*, 2020, **7**, 2292.
- 3 A. Nitti, R. Carfora, G. Assanelli, M. Notari and D. Pasini, *ACS Appl. Nano Mater.*, 2022, **5**, 13985.
- 4 J. A. Pomposo, *Single-Chain Polymer Nanoparticles: Synthesis; Characterization, Simulations, and Applications*, John Wiley & Sons, 2017.
- 5 J. A. Pomposo, *Polym. Int.*, 2014, **63**, 589.
- 6 A. Sanchez-Sanchez, A. Arbe, J. Colmenero and J. A. Pomposo, *ACS Macro Lett.*, 2014, **3**, 439.
- 7 H. Rothfuss, N. D. Knöfel, P. W. Roesky and C. Barner-Kowollik, *J. Am. Chem. Soc.*, 2018, **140**, 5875.
- 8 J. Rubio-Cervilla, E. González and J. A. Pomposo, *Nanomaterials*, 2017, **7**, 341.
- 9 T. Terashima, T. Mes, T. F. A. De Greef, M. A. J. Gillissen, P. Besenius, A. R. A. Palmans and E. W. Meijer, *J. Am. Chem. Soc.*, 2011, **133**, 4742.
- 10 A. Sanchez-Sanchez, A. Arbe, J. Kohlbrecher, J. Colmenero and J. A. Pomposo, *Macromol. Rapid Commun.*, 2015, **36**, 1592.
- 11 S. Thanneeru, J. Nganga, A. S. Amin, B. Liu, L. Jin, A. Angeles-Boza and J. He, *ChemCatChem*, 2017, **9**, 1157.
- 12 J. Chen, J. Wang, K. Li, Y. Wang, M. Gruebele, A. L. Ferguson and S. C. Zimmerman, *J. Am. Chem. Soc.*, 2019, **141**, 9693.
- 13 S. Garmendia, S. B. Lawrenson, M. C. Arno, R. K. O'Reilly, D. Taton and A. P. Dove, *Macromol. Rapid Commun.*, 2019, **40**, e1900071.
- 14 W. Xu, D. Xiang, J. Xu, Y. Ye, D. Qiu and Z. Yang, *Polym. Chem.*, 2021, **12**, 172.
- 15 W. Wang, J. Wang, S. Li, C. Li, R. Tan and D. Yin, *Green Chem.*, 2020, **22**, 4645.
- 16 A. Blazquez-Martin, E. Verde-Sesto, A. Arbe and J. A. Pomposo, *Angew. Chem., Int. Ed.*, 2023, **62**, e202313502.
- 17 K. Mundsinger, A. Izuagbe, B. T. Tuten, P. W. Roesky and C. Barner-Kowollik, *Angew. Chem., Int. Ed.*, 2024, **63**, e202311734.
- 18 S. Mavila, I. Rozenberg and N. G. Lemcoff, *Chem. Sci.*, 2014, **5**, 4196.
- 19 N. D. Knöfel, H. Rothfuss, P. Tzvetkova, B. Kulendran, C. Barner-Kowollik and P. W. Roesky, *Chem. Sci.*, 2020, **11**, 10331.
- 20 J. L. Bohlen, B. Kulendran, H. Rothfuss, C. Barner-Kowollik and P. W. Roesky, *Polym. Chem.*, 2021, **12**, 4016.
- 21 S. Gillhuber, J. O. Holloway, H. Frisch, F. Feist, F. Weigend, C. Barner-Kowollik and P. W. Roesky, *Chem. Commun.*, 2023, **59**, 4672.
- 22 T. Dang-Bao, D. Pla, I. Favier and M. Gómez, *Catalysts*, 2017, **7**, 207.
- 23 S. Kar, H. Sanderson, K. Roy, E. Benfenati and J. Leszczynski, *Chem. Rev.*, 2022, **122**, 3637.
- 24 J. Sherwood, F. Albericio and B. G. de la Torre, *ChemSusChem*, 2024, e202301639.
- 25 J. De-La-Cuesta and J. A. Pomposo, *ACS Omega*, 2018, **3**, 15193.
- 26 T. K. Claus, J. Zhang, L. Martin, M. Hartlieb, H. Mutlu, S. Perrier, G. Delaittre and C. Barner-Kowollik, *Macromol. Rapid Commun.*, 2017, **38**, 1700264.
- 27 R. Bag, D. Sar and T. Punniyamurthy, *Org. Lett.*, 2015, **17**, 2010.

